2009

Measurement of Charging and Discharging of High Resistivity Materials Spacecraft Materials by Electron Beams

Ryan Hoffman

Joshua L. Hodges

Jesse Hayes

JR Dennison
Utah State University

Recommended Citation
Ryan Hoffmann, Joshua L. Hodges, Jesse Hayes and JR Dennison, "Measurement of Charging and Discharging of High Resistivity Materials Spacecraft Materials by Electron Beams," Paper Number : AIAA-2009-0561, 47th American Institute of Aeronautics and Astronomics Meeting on Aerospace Sciences, Orlando, FL, January, 5-8, 2009.

Measurement of Charging and Discharging of High Resistivity Spacecraft Materials by Electron Beams

Ryan Hoffmann[1], Joshua L. Hodges[2], Jesse Hayes[3] and JR Dennison.[4]
Physics Department, Utah State University, Logan, UT, 84325

New instrumentation has been developed for *in situ* measurements of the electron beam-induced surface voltage of high resistivity spacecraft materials in an existing ultra-high vacuum electron emission analysis chamber. Design details, calibration and characterization measurements of the system are presented, showing sensitivity to a range of surface voltages from <1 V to >12000 V, with resolution <1 V. The spatial profile of the voltage across the sample surface was measured by sweeping small electrodes across the surface, using a paddle attached to a vacuum compatible stepper motor mounted within a hemispherical grid retarding field analyzer. These electrodes formed one end of a floating charge transfer probe that enabled measurements to be made by a standard electrostatic field probe external to the vacuum chamber. Surface voltage measurements were also made periodically during the electron beam charging process and as the surface discharged to a grounded substrate after exposure. Analysis of the measured curves provides information on the material electron yields and bulk resistivity.

Nomenclature

CF	=	voltage conversion factor
C_f	=	voltage sensor plate capacitance
C_s	=	sample capacitance
C_w	=	capacitance of EFTP wire and feedthrough
C_{WP}	=	witness plate capacitance
R_i	=	effective resistance to ground of EFTP
V_{offset}	=	probe offset voltage
V_p	=	measured electrostatic field probe voltage
V_s	=	sample voltage
$\dot{V}_{drift}$	=	probe voltage drift rate
Δt	=	elapsed time since EFTP calibration to ground
ε_r	=	relative dielectric constant
ρ	=	resistivity
σ_s	=	sample charge density
σ_w	=	witness plate charge density
τ	=	probe voltage RC decay time
τ_D	=	thin film sample charge decay time

I. Introduction

THIS paper describes the results of a project to design, build, calibrate and test a system to measure the surface charge on an insulator as a function of time and position *in situ* in a spacecraft charging vacuum test chamber. In this system, surface charge is created when an insulator is bombarded by fast moving electrons, depositing charge and creating secondary electrons which are emitted from the material. Deposited charge dissipates on relatively long time scales by charge transport through highly resistive materials to grounded substrates. Our novel system uses a

[1] Research Associate and Graduate Student, Physics Department, UMC 4415, AIAA Member.
[2] Research Associate, Physics Department, UMC 4415.
[3] Undergraduate Student, Physics Department, UMC 4415.
[4] Professor, Physics Department, UMC 4415, Senior Member.

capacitive sensor to measure the surface voltage without dissipating the sample charge using a non-contact electrostatic field probe method. The sensor electrodes form one end of a floating charge transfer probe that enables measurements to be made by a standard electrostatic field probe external to the vacuum chamber. Our probe can measure a wide range of surface voltage, is very compact, and can be swept across the sample using an *in vacuo* stepper motor to measure surface charge distributions on samples *in situ*. This design extends our measurement capabilities by allowing the surface voltage probe to fit within an existing hemispherical grid retarding field analyzer so that surface voltages can be measured on samples tested using the extensive source flux and emission detection capabilities of the spacecraft charging vacuum test chamber.

A detailed description of the surface voltage probe (SVP) and electrostatic field transfer probe (EFTP) are provided. We emphasize how the sensor is incorporated into the existing detector. An overview of the main electron emission chamber is included to illustrate the full capabilities of the surface voltage test system.

We describe measurements to characterize the stability, sensitivity, accuracy, range, spatial resolution and temporal response of the surface charge measurable by our system. Two measurements are also described to illustrate the research capabilities of the test system. The spatial profile of the voltage across the sample surface was measured by sweeping a small electrode across the surface. Surface voltage measurements were also made periodically during the electron beam charging process and as the surface voltage discharged to a grounded substrate after exposure. Analysis of the measured curves provides information on the material electron yields and bulk resistivity. Applications to studies by our group of electron emission from insulators and conductors, as well as spacecraft charging, are also discussed.

II. Instrumentation

A. Overview of Electron Emission Test Chamber

The primary instrument of the Utah State University (USU) test facility to study electron emission from conductors and insulators is a versatile ultra-high vacuum (UHV) chamber with surface analysis and sample characterization capabilities. This system is described in more detail elsewhere.[1-7] This chamber can simulate diverse space environments including controllable vacuum ($<10^{-10}$ to 10^{-3} Torr) and ambient neutral gases conditions, temperature (<150 to >400 K), as well as sources for a broad range of electron, ion and photon fluxes and energies. A variety of detectors are available for measurements of single or simultaneous electron-, ion-, and photon-induced emission,[2,4,5] including a standard Faraday cup detector, hemispherical analyzer, cylindrical mirror, and time of flight micro-channel plate detector. Specifically, they allow us to measure total emitted electron (ion) yield, backscattered/secondary yield, charge decay curves, and energy spectra.[1]

Two primary electron sources provide monoenergetic electron beams ($\Delta E/E<2\cong10^{-4}$) with electron energy ranges from ~20 eV to ~25 keV and incident electron currents ranging from 0.1 nA to 10 :A, beam spot diameters ranging from ~50 μm to >10 mm (depending on beam energy), and pulsing capabilities ranging from 10 ns to continuous emission. The low energy electron gun (Staib, Model NEK-050-SP) is operated at incident electron energies of ~20 eV to 5000 eV with a typical beam current of ~ 10 nA and a typical ~3 mm diameter beam spot. The high energy electron gun (Kimball, Model EGPS-21B) is operated at incident electron energies of 5 keV to 25 keV with a typical beam current of ~20 nA and a typical 500 μm diameter beam spot. Stable, uniform, well-characterized beam fluxes of 0.05 nA-cm^{-2} to 150 nA-cm^{-2} or higher are possible from the electron guns. There are also three ion guns with <0.1 to 5 keV monoenergetic sources for inert and reactive gases; one (PHI, Model I11-065) has rastering and pulsed deflection capabilities. The NIR-VIS-UV solar irradiance spectrum is simulated using a pair of pulsed, monochromated lamp sources: (i) a Tungsten/halogen lamp system with a *Suprasil* envelope produces focused (~0.5 cm diameter) radiation from 0.4 eV to 7.2 eV (200 nm to 2000 nm) and (ii) a Deuterium RF powered continuum source with a MgF_2 window produces focused (~0.5 cm diameter) radiation from 3.1 eV to 11.1 eV (150 nm to 400 nm). Additional light sources include a helium resonance lamp (21.2 and 40.8 eV), broadband Hg discharge and W-filament sources, and a variety of quasi-monochromatic NIR/VIS/UVA LED sources.[1]

For conducting samples, electron guns are operated using a continuous, low-current beam of electrons, and dc-currents are measured with standard ammeters sensitive to tens of picoamperes. The system at USU to measure electron emission from insulators uses a combination of methods to control the deposition and neutralization of charge. Typically, charge deposition is minimized by using a low current beam (~10-30 nA) focused on a sample area of ~7 mm^2 that is delivered in short pulses of ~5 μsec. Each pulse contains ~150 fC or ~10^5 electrons-mm^{-2}. For a typical ~100 μm thick dielectric sample, this amount of charge is estimated to change the surface potential by only 10-100 mV/pulse (positive) and requires ~500 pulses/sec to achieve an ~1 nA/cm^2 dosage that typically causes discharge in space. The pulsed system uses custom detection electronics developed at USU with fast (1-2 μs rise

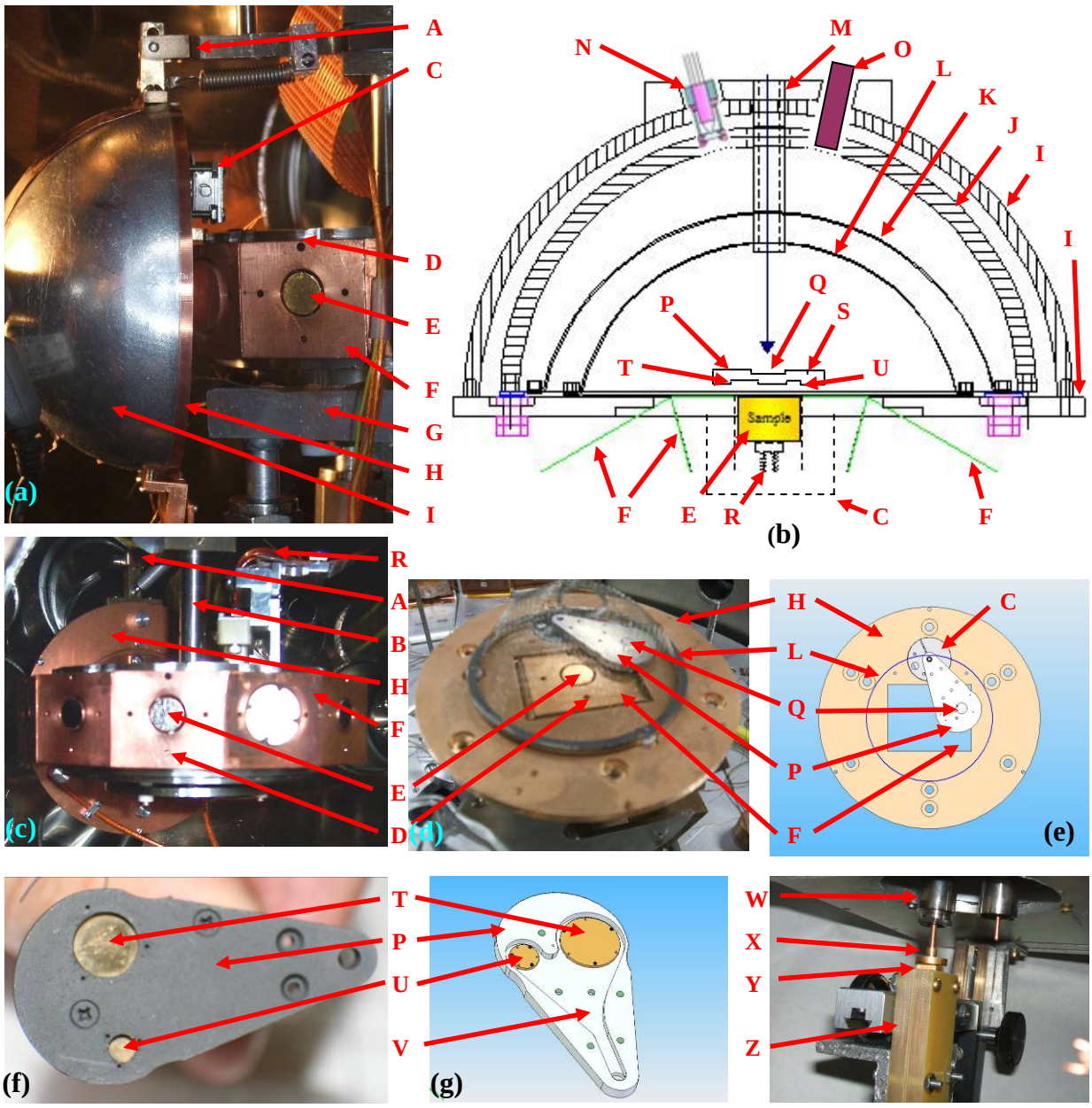

Figure 1. Hemispherical Grid Retarding Field Analyzer (HGRFA) and Surface Voltage Probe (SVP). ***(a)*** *Sample stage and HGRFA detector (side view).* ***(b)*** *Cross section of HGRFA.* ***(c)*** *Sample stage and HGRFA detector shown without* ***C*** *and* ***G*** *(front view).* ***(d)*** *Interior view of the partially assembled HGRFA showing sample block and inner grid.* ***(e)*** *Diagram of HGRFA interior with SVP.* ***(f)*** *Surface voltage probe assembly.* ***(g)*** *Diagram of SPV interior and Au electrodes.* ***(h)*** *Ex situ portion of Electrostatic Field Transfer Probe (EFTP) assemble.*

LEDGEND

A *HGRFA Hinged Mount*	***I*** *HGRFA Hemispherical Shield*	***R*** *Sample Current Lead*
B *Sample Carousel/HGRFA Rotation Shaft*	***J*** *HGRFA Collector*	***S*** *SVP Faraday Cup*
	K *HGRFA Bias Grid*	***T*** *SVP 7 mm Diameter Au Electrode*
C *UHV Stepper Motor*	***L*** *HGRFA Inner Grid*	***U*** *SVP 3 mm Diameter Au Electrode*
D *Sample Block Faraday Cup*	***M*** *HGRFA Drift Tube*	***V*** *SVP Wiring Channel*
E *Sample (10 mm)*	***N*** *Electron Flood Gun*	***W*** *EFTP Vacuum Feedthrough*
F *Sample Block*	***O*** *LED Light Source*	***X*** *EFTP Witness Plate*
G *Cryogen Reservoir*	***P*** *Surface Voltage Probe (SVP)*	***Y*** *Electrostatic Field Probe*
H *HGRFA Face Plate*	***O*** *Au disc Electron Emission Standard*	***Z*** *Probe XYZ Translator*

time) sensitive/low noise (10^7 V/A / 100 pA noise level) ammeters for determining insulator emission with minimal charging effects.[4,5] Detected current pulses from the ammeters are sent to a fast (100 MHz, 1 GS/s) digital storage oscilloscope (Tektronics Model TDS 2014). Charge dissipation techniques include a custom low energy (~1-10 eV) electron flood gun for direct neutralization of positively charged surfaces between incident pulses.[4,5,8] A variety of visible and UV light sources are used for neutralization of negatively charged surfaces through the photoelectric effect. Sample heating to ~50-100 °C has also been used for dissipation of buried charge by thermally increasing the sample conductivity. Often, samples will be heated to ~50 °C over night to increase conductivity and dissipate charge after a day of electron emission measurements. Both DC and pulsed measurements and data retrieval are fully computer automated, using GPIB interfacing and a DAQ card under LabVIEW™ control. A complete description of the DC-system and pulsed-system setups, along with additional insulator-yield and charging data, is available in other references.[2-5]

B. Detector and Sample Assembly

The primary detector for emission studies is a custom hemispherical grid retarding field analyzer (HGRFA), with a retarding-field analyzer grid system for emitted-electron energy discrimination between back scattered electrons (energies >50 eV) and secondary electrons (energies <50 eV) (see Figure 1). By ramping the grid (refer to labels **K** and **L** in Figure 1) bias, energy spectra of the emitted electrons can also be measured using this detector. The HGRFA features an aperture and drift tube (**M**) for incident electron/ion admission and a fully-encasing hemispherical collector (**J**) for full capture of emitted electrons, that is particularly well suited and calibrated for absolute yield measurements.[2,3,5] The hemispherical grid detection system has been carefully calibrated (both through calculation and measurement) to account for detector losses, allowing yield accuracies of better than 2% for conductor yields and better than 5% for insulator yields.[1,2] The HGRFA can be independently positioned in front of any sample (see Figure 1(c)). A low energy flood gun (**N**) and a variety of visible and UV LED light sources (**O**) are mounted on the HGFRA housing at near-normal incidence to provide neutralization of surface charging between pulses. A collimating lens mounted on the HRFA and attached to a fiber optic cable and vacuum feedthrough allow external light sources to be used or a photospectrometer to analyze emitted light from the sample. The flood gun (**N**) also acts as a low energy (~1eV to 100 eV) focused electron source.

Samples (**E**) are mounted on (10.0 ± 0.1) mm diameter Cu cylinders, usually using a Cu tape with conductive, UHV-compatible adhesive routinely used for scanning electron microscope studies (3M, Type 1182 tape). The Cu cylinders are mounted in sample blocks (**F**) on the sample carousel, using ceramic pins to provide electrical isolation. Electrical connection to the sample is made via a spring loaded pin (**R**) from the rear, allowing the current to the sample to be monitored. The sample carousel has eleven sample blocks that can be rotated in front of the various flux sources. Typically, one sample block contains a photodiode, another a Faraday cup, and a third a Au sample as an electron emission standard (see Figure 1(c)).

C. Surface Voltage Probe Design

The surface voltage probe (SVP) is a small device that fits within the HGRFA to measure the surface potential of a sample. Figure 1(f) shows the assembled SVP, which is <40 mm long and only ~21 mm wide, with a thickness of <3 mm. Two openings in the casing of 7.0 mm (**T**) and 3.0 mm (**U**) diameter define the effective electrode areas. The casing is coated with colloidal graphite to minimize the production of secondary electrons by stray electrons inside the HGRFA (see Figure 1(f)). There are two electrodes on the sample side of the sensor ~50 μm above the sample surface, each kinematically positioned by three 76 μm diameter sapphire spheres above and below the electrodes ($\rho > 10^{18}$ Ω-cm). The electrodes are very well electrically isolated from the outer casing of the unit by the sapphire spheres. The electrodes are Au plated to minimize surface contamination and allow a uniform charge density on the probe. Currents to the two electrodes, the Au disc, and the full SVP casing can be monitored independently because each are electrically isolated. The two voltage sensor plates (**U** and **T**) are each connected separately to external witness plates (**X**) by ~1 m of thin 200 μm diameter magnon wire with very thin insulation to minimize the capacitance of the EFTP. Two 4 mm x 15 mm diameter Au plated external witness plates (**X**) are mounted on an ultrahigh high vacuum compatible dual floating MHV feedthrough (MDC Model MHV-275-2) (**W**). The sensor of the electrostatic field probe (Monroe Electronics Isoprobe Model 162) (**Y**) is mounted on precision XYZ translation stage (**Z**) to precisely position the probe in front of one or the other witness plates with a ~250 μm probe to plate separation. The electrostatic field probe control electronics (Monroe Electronics Model 1017AEL) can measure surface voltage of -10 V to + 10 V with a resolution of 1 mV. Provisions have been made to alternately mount another electrostatic field probe (Trek Model 341 A) that can measure surface voltages of -20 kV to + 20 kV with ~0.5 V resolution to measure higher sample voltages.

The SVP is mounted on a small sized (~25 mm x 11 mm diameter), ultra-high vacuum-compatible stepper motor (Attocube Systems, Model ANR50res) (**C**). The microstepper controller (Model ANC200), with a resistive position encoder, provides rapid and extremely fine (<1 m° per step) positioning. The SVP can be positioned on either side of the sample providing an unobscured view for the incident beam and can be swept from side to side allowing either electrode to pass fully over the sample.

Positioning the SVP inside the HGRFA has several advantages. The primary advantage is that surface voltage measurements can be made rapidly, while the sample and HGRFA are accurately aligned with the incident beam. In addition, an electrically isolated 10 mm diameter Au disc (**O**) is mounted on the source side of the probe and can be swung into place above the sample in line with an incident beam. Doing so provides a Au electron emission calibration standard for the detector without the need of moving the HFGRA above the Au sample mounted in the sample block and moving this sample block in line with the incident beam. Further, the SVP in this position can act as a shield for the sample preventing any stray electrons or light from charging or discharging the sample. There is also a 360 μm diameter Faraday cup (**S**) in the source side of the probe that can be swept across the sample to characterize the incident beam profile and provide an accurate measure of the incident flux.

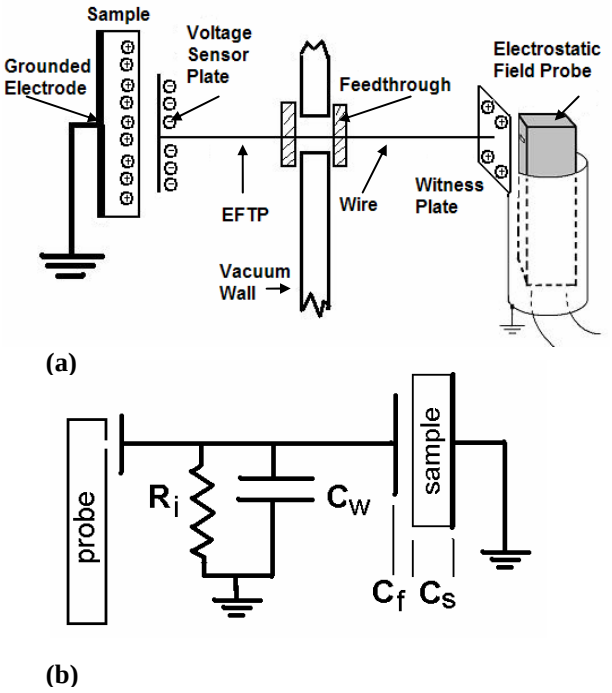

Figure 2. Schematic of the EFTP assembly. ***(a)*** *Charge distribution for the EFTP assembly. Shown are the sample (left), EFTP (center), and electrostatic field probe, (right). (b) Effective circuit for EFTP.*

D. Electrostatic Field Transfer Probe Design

The EFTP (Electrostatic Field Transfer Probe) used here is based on Frederickson's idea that a transfer probe can induce a surface voltage on an external witness plate proportional sample surface voltage, that can be easily measurable outside of the vacuum.[12,13] The EFTP consists of a voltage sensor plate positioned above the sample (one of the surface voltage probe electrodes (**U** or **T**)) connected by a low-capacitance wire to an external witness plate (**X**) positioned outside the vacuum chamber close to a standard electrostatic field probe (**Y**) (see Figure 2(a)).

To accurately measure a surface voltage, the sample plate and witness plate are positioned adjacent to grounded surfaces and the EFTP is grounded. This assures that there in on net charge on the EFTP and that the charge density is zero on both plates. The EFTP is then disconnected from ground and the witness plate voltage is measured with the electrostatic field probe; this provides a measure of the zero offset, V_{offset}. A known voltage is then placed on a conducting sample. This causes an equal magnitude and opposite polarity charge density to form on the voltage sensor plate. However, since there is still no net charge on the EFTP (assuming that the probe is fully isolated), an equal magnitude charge is found at the opposite end of the EFTP. The charge density on the witness plate, σ_w, is then of the same polarity as the sample charge density, σ_s, with magnitude of the witness plate charge density scaled by the ratio of the voltage sensor plate capacitance to witness plate capacitance, $\sigma_w=(C_f/C_{WP})\sigma_s=CF\cdot\sigma_s$. The proportionality constant, CF, depends on the plate areas and separations, but can be determined directly by measuring the witness plate voltage with the external electrostatic field probe for a variety of applied sample voltages. Once calibrated, the EFTP can then be used to measure unknown surface voltages or charge densities of conducting or insulating samples.

More correctly, one must consider the coupling of the EFTP to ground, including both the capacitance of the wire and probes and the leakage resistance to ground through the feedthrough, wire insulation, and probe mounts.[9] Figure 2(b) shows an equivalent circuit, where C_w is the wire and feethrough capacitance, R_i is the leakage resistance of the EFTP, and C_f is the capacitance of the sample surface to the voltage sensor plate. For a voltage on the sample, V_s (or equivalently a charge $Q_s=C_s\cdot V_s$, where C_s is the capacitance of the sample surface to both the voltage sensor plate and ground), the electrostatic field probe will read a voltage

$$V_s = \left(\frac{C_W + C_f}{C_f} \right) V_{p_o} e^{-t/\tau} \qquad with \quad \tau = R_i C_W \tag{1}$$

The initial probe voltage V_{po} decays with time as charge leaks into (or from) the EFTP, with an RC time constant, τ. The value of R_i is actually only an effective resistance, since decay occurring initially is primarily a result a displacement current due to the capacitor polarization and only later due to a resistive current due to charge leakage.

There are distinct advantages in using the EFTP and having the electrostatic field probe outside the vacuum chamber. Others have measured the surface voltage directly with electrostatic field probes inside the vacuum chamber and adjacent to the sample;[14,15] however, these methods were often subject to problems.[9,10] The required proximity of the electrostatic probe to the sample means that stray electron beam radiation—from secondary scattering scattering, insufficient beam columniation, or beam rastering—can charge the sensitive electrostatic probe, often driving it off scale. Because it is difficult to discharge a probe in the vacuum, this can lead to large, unpredictable and persistent voltage offsets and can even damage the probe that can not be readily repaired *in vacuo*.

Another reason for preferring the EFTP arrangement relates to electron emission from insulators.[11] Electron beam charging of the samples produces an electric field at the surface of the sample that can drive electrons out of the surface. While penetrating into the insulator, the high-energy electrons excite electrons and holes into trapping states and into mobile states located in the region between the sample surface and the maximum depth of penetration. Such conducting species provide the charge to be later emitted from the surface. An *in situ* electrostatic field probe can collect these emitted electrons, thereby altering the net charge on the electrostatic field probe and affecting the voltage reading.

The same modification of the net charge on the EFTP can occur for *ex situ* electrostatic field probes. However, by knowing the capacitance, C_f, the rate of voltage change on the voltage sensor plate provides a direct, sensitive method to determine the electron currents leaving the sample surface. After establishing V_{offset} when the sensor field plate faces ground, the sample is rotated before the sensor and held there for a period of time, ***t***. The measured voltage will change both because current is emitted to the sensor field plate and because the sample voltage is decaying. After the sensor field plate has collected charge, it is again faced to ground and its new V_{offset} reading shows how much charge was absorbed during time ***t***. Measurements of the decay of surface voltage, performed rapidly so that negligible charge is delivered to the sensor plate, provides independent information about the total loss of charge from the sample. Subtracting the emitted charge from the total charge loss provides the charge conducted through the sample to the grounded electrode.

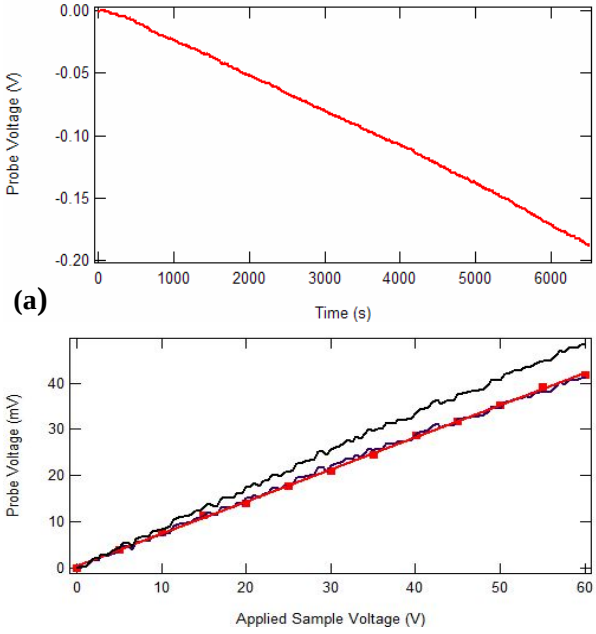

Figure 3. EFTP calibration tests. (a) *Time dependant probe voltage drift for an applied sample voltage of 0 V, with a slope of (28.97±0.04) $\mu V_p/s$.* **(b)** *Voltage calibration of probe voltage to an applied sample voltage. Red symbols are for data taken at 5 V and ~3 s intervals over ~1 min. The black curve is for data measured at 0.5 V and ~6 s interval over ~12 min. The blue curve shows data from the black curve after a linear correction for voltage drift. The red curve is a linear fit to the corrected data with a slope of (666±4) $\mu V_p/V_s$ and an intercept of (3.5±0.5) μV_p.*

III. Calibration and Characterization

To calibrate the EFTP drift due to leakage, a constant voltage was placed on the sample and the probe voltage was monitored with time over ~2 hr, as shown in Figure 3(a). The voltage was found to change almost linearly with time at a rate of $\dot{V}_{drift}$=(28.97±0.04) μV/s. Measurements made for nonzero applied voltages produced very similar drift rates. Without correcting for voltage drift, there would be a ~0.5 V error in measured surface voltage, comparable to the instrument resolution, in ~ 12 s.

After correcting for a linear drift, measurements can be taken for > 4 hr with <20 V error.

To determine the calibration factor of the EFTP, measurements were made of the probe voltage for a series of known sample voltages, as shown in Figure 3(b). An initial set of surface voltages were taken rapidly at 5 V and ~3 s intervals over ~1 min. These data exhibited a highly linear dependence with a calibration factor of CF=(1.502±0.009) $V_s/\mu V_p$ and an offset voltage of V_{offset}=(3.5±0.5) μV_p. A second set of data was taken more slowly at 0.5 V and ~6 s interval over ~12 min. These data had a somewhat larger slope due to voltage drift. However, when corrected for a linear drift, the longer duration data set agreed very well with the shorter duration data set. The calibration factor was also found to agree very well over a range of applied voltages up to 300 V. Tests also indicated that an accurate surface voltage measurement could be made in <500 ms, as limited by the time constant of the EFTP (~100 ms), the response time of electrostatic field probe (<5 ms), and data acquisition time.

The probe offset voltage, typically on the order of a few mV, was found to differ for each test and must be measured for each test sequence by performing an applied voltage calibration run. It is also good practice to determine the calibration factor for each set of experiments as well, as there is some small variation due to specific sample and sensor conditions and separation.

Combining the results of the calibration tests, the measured probe voltage is related to the actual surface voltage:

$$V_s(\Delta t) = CF \cdot \left[V_p + \dot{V}_{drift} \cdot \Delta t + V_{offset} \right] \tag{2}$$

where Δt is the elapsed time since recalibration of the probe to a grounded surface. Based on the calibration and test measurements, the EFTP and SVP assembly were found to work well. The unit was sensitive to a surface voltage of <1 V with a resolution of ~0.5 V. Surface voltages up to ±12 kV could be measured with the Monroe probe. Much higher voltages could be measured with a Trek electrostatic field probe that can in principle monitor probe voltages up to ±20 kV. A modest voltage drift rate was observed in the sample voltage of <3 mV_s/sec. Without correction for drift, surface voltages can be measured for short periods of time—long enough for accurate surface sweeps—between recalibration of the probe. With a linear voltage drift correction, surface voltages can be measured to high accuracy for periods >4 hr between probe recalibration. Measurements of a grounded sample voltage were stable over hours to ~0.1 V after correcting for a linear voltage drift and initial V_{offset}.

IV. Typical Measurements

Two sets of data were acquired for a charged, highly insulating sample to illustrate the capabilities of the new test system. The polyimide sample was a 25 µm thick film of Kapton HN from Dupont.

A. Sweep

The spatial profile of the voltage across the sample surface, shown in Figure 4(a), was measured by sweeping the 7.0 mm diameter Au voltage sensor electrode (**T**) over a 10.0 mm diameter uniformly charged polyimide sample (**E**). The shape of the voltage profile is consistent with the convolution of a sensor disc with a uniformly charged sample disc. The spatial resolution for the larger diameter probe after deconvolution is estimated to be 1 mm to 2 mm. Preliminary measurements with the 3 mm diameter Au voltage sensor (**U**) indicate a better spatial resolution, on the order of 0.5 mm to 1 mm.

Measurements of the charge distribution on a polyimide sample from a focused, ~3 mm diameter electron beam demonstrated the capability of measuring nonuniform charge distributions on the sample. More such measurements are in progress, including ones to

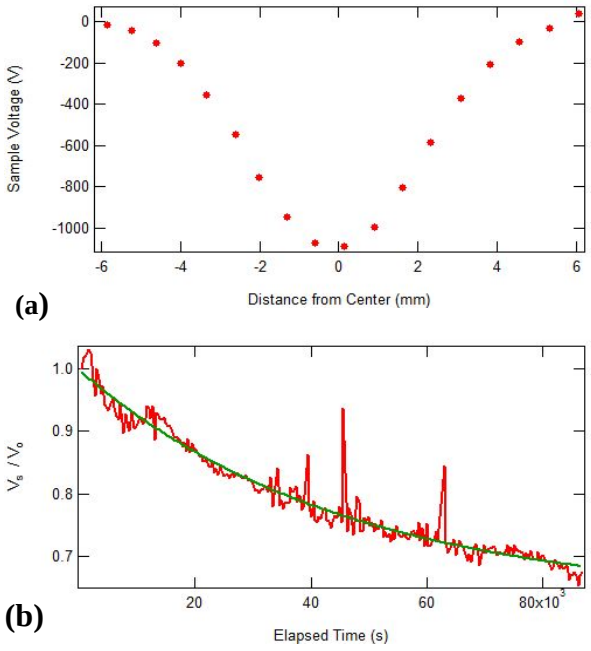

Figure 4. Flipper measurements. ***(a)*** *Sweep of 7.0 mm diameter Au voltage sensor electrode over a 10.0 mm diameter uniformly charged polyimide sample.* ***(b)*** *Temporal decay of normalized surface voltage of a charged polyimide sample. The fit is an exponential decay with a time constant of (6.0±0.3)·10^3 s.*

correlate the nonuniform charge distribution with a beam profile measured with a Faraday cup sensor and to monitor the lateral spread of the surface charge from a focused beam spot with time.

B. Decay

Surface voltage profile measurements were made periodically during the electron beam charging process and as the polyimide sample discharged to a grounded substrate after exposure. The total dose of $9 \cdot 10^{-13}$ C (<1 pA-cm^{-2}) was delivered in approximately ten 5 μs pulses over ~30 min. The discharge curve is shown in Figure 4(b). An exponential decay with a time constant of τ_D=(16.7±0.8) hr provides a good fit to the long term data. Assuming that the charge all decays through ohmic conduction through the polyimide film to the grounded substrate, the resistivity of the polyimide $\rho = \tau_D/\varepsilon_o\varepsilon_r$ is ~$2 \cdot 10^{17}$ Ω-cm assuming a relative dielectric constant, ε_r, of 3.40. This is a factor of ~30 lower than the resistivity of Kapton measured by the charge storage method, $6 \cdot 10^{18}$ Ω-cm.[13]

Measurements are in progress to study voltage decay curves for additional materials, to determine dark current resistivities for various materials, and to study decays for longer periods of time. We are studying the voltage decay curves and their relation to determination of the "intrinsic" yields for highly insulating materials subject to charging by low-fluence probe beams.[7] We are also studying the initial rise in surface voltage often observed (see Figure 4(b)) to test its reproducibility and to determine if the effect is related to migration of internal charge layers or to post-irradiation electron emission.

Acknowledgments

We gratefully acknowledge the fundamental inspiration, useful discussions and encouragement of Robb Frederickson. Prasanna Swaminathan also was instrumental in developing the use of the EFTP at USU. This work was supported by a project for the James Web Space Telescope Electrical Systems Group through the NASA Goddard Space Flight Center.

References

[1]J.R. Dennison, C.D. Thomson, J. Kite, V. Zavyalov, Jodie Corbridge, "Materials Characterization at Utah State University: Facilities and Knowledgebase of Electronic Properties of Materials Applicable to Spacecraft Charging," *Proceedings of the 8th Spacecraft Charging Technology Conference*, Huntsville, Alabama, 2003.

[2]Neal Nickles, "The Role of Bandgap in the Secondary Electron Emission of Small Bandgap Semiconductors: Studies of Graphitic Carbon," PhD Dissertation, Physics Dept,. Utah State University, 2002.

[3]W.Y. Chang, J.R. Dennison, Neal Nickles and R.E. Davies, "Utah State University Ground-based Test Facility for Study of Electronic Properties of Spacecraft Materials," *Proceedings of the 6th Spacecraft Charging Technology Conference*, Air Force Research Laboratory Science Center, Hanscom Air Force Base, MA, 1999.

[4]C.D. Thomson, V. Zavyalov, J.R. Dennison, "Instrumentation for studies of electron emission and charging from insulators," Proc. of 8th Spacecraft Charging Technology. Conf., Huntsville, Alabama, 2003.

[5]C.D. Thomson, "Measurements of the Secondary Electron Emission Properties of Insulators", Ph.D. Dissertation, Physics Dept., Utah State Univ., 2004.

[6]J.R. Dennison, Alec Sim and Clint Thomson, "Evolution of the Electron Yield Curves of Insulators as a Function of Impinging Electron Fluence and Energy," *IEEE Transaction on Plasma Science,* Vol. 34, No. 5, October 2006, pp. 2204-2218.

[7]Ryan Hoffmann, JR Dennison Clint D. Thomson and Jennifer Albresten, "Low-fluence Electron Yields of Highly Insulating Materials" *IEEE Transaction on Plasma Science,* Vol. 36, No. 5, October 2008, pp. 2238-2245.

[8]I. Krainsky, W. Lundin, W.L. Gordon, and R.W. Hoffman, Secondary Electron Emission Yield Annual Report for Period July 1, 1979 to June 30, 1980, Case Western Reserve University, Cleveland, OH, 1980 (unpub.).

[9]Prasanna Swaminathan , "Measurement of Charge Storage Decay Time and Resistivty of Spacecraft Insulators," MS Thesis, Electrical and Computer Engineering Department; Utah State University, 2004.

[10]Prasanna Swaminathan, A. R. Frederickson, J.R. Dennison, Alec Sim, Jerilyn Brunson, Eric Crapo, "Comparison Of Classical And Charge Storage Methods For Determining Conductivity Of Thin Film Insulators," *Proc. of 8th Spacecraft Charging Technology Conf.*, , Huntsville, Alabama, October 20-24, 2003.

[11] A.R. Frederickson and J.R. Dennison, "Measurement of Conductivity and Charge Storage in Insulators Related to Spacecraft Charging," *IEEE Transaction on Nuclear Science*, Vol. 50, No. 6, December 2003, pp. 2284-2291.

[12]A.R. Frederickson and J.R. Dennison, "Measurement of Conductivity and Charge Storage in Insulators Related to Spacecraft Charging," *IEEE Transaction on Nuclear Science*, Vol. 50, No. 6, 2003, pp. 2284-2291 [13]A.R. Frederickson, C. E. Benson and J. F. Bockman, "Measurement of Charge Storage and Leakage in Polyimides," *Nuclear Instruments and Methods in Physics Research B*, 454-60, 2003.

[14]L. Levy, D. Sarrail, and J. M. Siguier, "Conductivity and secondary electron emission properties of dielectrics as required by NASCAP," *Third European Symposium on Spacecraft Materials in Space Environment*, 1993, pp. 113-123.

[15]R. Coelho, L. Levy, and D. Sarrail, "Charge decay measurements and injection in insulators," *Journal of Applied Physics*, Vol. 22, No. 9, Sept. 1989, pp. 1406-1409.